https://doi.org/10.1016/j.renene.2018.11.042



# Altering the chemical state of boron towards the facile synthesis of $LiBH_4$ via hydrogenating lithium compound-metal boride mixture

Weitong Cai[1,*], Jianming Hou[2], Shiyong Huang[1], Juner Chen[3], Yuanzheng Yang[1], Pingjun Tao[1], Liuzhang Ouyang[4,5], Hui Wang[4,5], Xusheng Yang[6,*]

[1] *School of Materials and Energy, Guangdong University of Technology, Guangzhou, 510006, China*

[2] *Department of Mechanical and Electrical Engineering, Guangdong Polytechnic of Environmental Protection Engineering, Foshan, 528216, China*

[3] *Department of Chemistry, Zhejiang University, Hangzhou, 310027, P. R. China*

[4] *School of Materials Science and Engineering, South China University of Technology, Guangzhou 510640, China*

[5] *Guangdong Provincial Key Laboratory of Advance Energy Storage Materials, South China University of Technology, Guangzhou, 510640, China*

[6] *Department of Industrial and Systems Engineering, The Hong Kong Polytechnic University, Hung Hom, Kowloon, Hong Kong, China*

Declarations of interest: none

* Corresponding author:
Weitong Cai
E-mail: mewtcai@gdut.edu.cn
Xusheng Yang
E-mail: xsyang@polyu.edu.hk

Coauthors:
Jianming Hou
E-mail: ben0413@163.com
Juner Chen
E-mail: jrchen@zju.edu.cn
Yuanzheng Yang
E-mail: yangyz@gdut.edu.cn
Pingjun Tao
E-mail: pjtao@gdut.edu.cn
Liuzhang Ouyang
E-mail: meouyang@scut.edu.cn
Hui Wang
E-mail: mehwang@scut.edu.cn

**Abstract**

Boron sources in forms of $SiB_4$/FeB/$TiB_2$ were used to react with LiF/LiH under hydrogen atmosphere to investigate their effectiveness for synthesizing $LiBH_4$, a promising hydrogen storage material. Fourier transform infrared (FTIR) study revealed the formation of B-H bond vibrations in these hydrogenated systems, and it demonstrated the generation of $LiBH_4$. When using FeB and $TiB_2$, few amounts of B-H bonds were formed in the hydrogenated samples either reacting with LiH or LiF. When utilizing $SiB_4$, the formation of B-H bonds was promoted for both systems mixing with LiH and LiF. The results imply that a stepwise process of $LiBH_{4-x} \rightarrow LiBH_4$ possibly took place during the hydrogenation process. Importantly, $SiB_4$-LiH system exhibited the best hydrogenation performance. At moderate conditions of 250 ºC and 10 MPa $H_2$, $LiBH_4$ was successfully synthesized from this system. A facile synthesis pathway, $SiB_4(s) + 4LiH(s) + 6H_2(g) \rightarrow 4LiBH_4(s) + Si(s)$, having a $\Delta_r H_m$ of -65 kJ/mol $H_2$, was proposed. This study supports that the chemical state of boron in the reactant is an important factor affecting the generation of $LiBH_4$. A hydrogenation reaction between $SiB_4$ and $CaH_2$ or $MgH_2$ may be also applicable for synthesizing $Ca(BH_4)_2$ or $Mg(BH_4)_2$, which are regarded as potential hydrogen storage materials.

Keywords: hydrogen storage, hydrogenation, boride, borohydride, $LiBH_4$

## 1. Introduction

Nowadays, hydrogen has already been regarded as an ideal secondary energy due to its high energy density and non-pollution, and the considerable exploitation of shale gas will certainly enhance the hydrogen production through methane reforming technology[1, 2]. However, hydrogen storage is one of the major challenges for hydrogen energy application especially for on-board or off-board fuel cell vehicles[3].

Solid-state hydrogen storage materials with high capacities, such as magnesium hydride, alanates, amides, and borohydrides, unfold an efficient and safe hydrogen storage technology[4-6]. Lithium borohydride ($LiBH_4$) is regarded as a promising candidate for advanced hydrogen storage because of its high hydrogen storage capacity of 18.4 wt.% and 121 $kg/m^3$[2]. One envisaged difficulty is how to synthesize $LiBH_4$ through a facile approach to spread its wide utilization as hydrogen storage material[7]. Conventionally, $LiBH_4$ is industrially synthesized through a metathesis reaction between $NaBH_4$ and lithium halide, and isopropylamine or tetrahydrofuran was used as solvent to extract $LiBH_4$ product, as shown in equation (1)[8].

$$NaBH_4(s) + LiCl(s) \rightarrow LiBH_4(s) + NaCl(s) \quad (1)$$

$$B_2H_6(g) + 2LiH(s) \rightarrow 2LiBH_4(s) \quad (2)$$

However, $NaBH_4$, an expensive material, should be prepared before the metathesis reaction procedure was carried out. Recently, gas-solid synthesis approach via a reaction between solid compound(s) and hydrogen source is proposed as a promising way. Great efforts have been paid to the "hydroboration" approach by reacting diborane ($B_2H_6$) with lithium hydride (LiH), as shown in equation (2)[9]. Because B-H bonds had been established already in a form of $B_2H_6$, the reaction pathway, therefore, could facilitate the formation of $LiBH_4$ at lower temperatures and pressures.

Friedrichs et al. demonstrated the formation of $LiBH_4$ by heating LiH in $B_2H_6$ atmosphere at 120 °C and a yield of 72 wt.% $LiBH_4$ was achieved at 185 °C[10]. The authors also found that a higher yield could be achieved by a ball milling treatment of the materials[11, 12]. And, a reaction mechanism was proposed between LiH and $B_2H_6$[9]. The "hydroboration" approach was also useful to synthesize other light-weight complex hydrides, such as $Ca(BH_4)_2$, $Mg(BH_4)_2$ and $Y(BH_4)_3$, etc.[12, 13]. However, a beforehand synthesis of $Zn(BH_4)_2$ or $LiZn_2(BH_4)_5$ as a source of $B_2H_6$ through a chemical reaction between $LiBH_4$ and $ZnCl_2$ consumes more material resources and input energy. Besides, the high toxicity and thermodynamic instability of $B_2H_6$ gas further restrict the large-scale utilization of this "hydroboration" approach[10, 11].

An alternative way is hydrogenation, which directly exposes the materials in hydrogen gas under certain pressures and temperatures. Chen et al. found that extremely harsh conditions of 400 °C and 35 MPa were necessary for hydrogenating the mixture of LiH and B into $LiBH_4$[14-16]. Friedrichs et al. reported that $LiBH_4$ was directly synthesized from the Li and B mixture, $LiB_3$ or $Li_7B_6$ compound under 700 °C and 15 MPa $H_2$, and $LiBH_4$ started to form at 350 °C in the case of $LiB_3$[17, 18]. Çakanyıldırım et al. reported that the optimal stoichiometric ratio of B to Li was 0.214 for generating 90 wt.% $LiBH_4$ easily by leaving LiB compound in 6 MPa hydrogen[19]. Recently, great interest has been focused on a typically reversible system of $MgB_2$-LiH[20]. When a temperature of 300 °C and a hydrogen pressure of 20 MPa were applied to the $MgB_2$-LiH mixture, $LiBH_4$ was confirmed in the hydrogenated product[21]. By prolonging the milling time from 24 h to 120 h for the mixture, the hydrogenation parameters were remarkably optimized resulting in lower conditions of 265 °C and 9 MPa $H_2$[22]. Besides, by introducing Ti-based additives, the hydrogenation performance of $MgB_2$-LiH was further

enhanced showing lower temperature and pressure, e.g., 256 °C and 5 MPa[23-25]. The systems of $MgB_2$-LiF or $MgB_2$-LiH-LiF also demonstrated their feasibility of synthesizing $LiBH_4$ under hydrogenation conditions of 390 °C and 6 MPa, and their reaction pathways strongly depended on the reactant's stoichiometric ratio[26-28]. Table 1 shows the synthesis conditions of several typical $LiBH_4$ systems through gas-solid reaction.

Enlightening by these studies, hydrogenation treatment of lithium compound-metal boride system suggests its capability for synthesizing $LiBH_4$. In this work, the feasibility of $SiB_4$/FeB/$TiB_2$-LiF/LiH systems was investigated, and $LiBH_4$ was successfully synthesized from $SiB_4$-LiH system at moderate hydrogenation conditions of 250 ºC and 10 MPa.

Table 1 Synthesis conditions of several typical $LiBH_4$ systems through gas-solid reaction

| No. | System | Temperature (°C) | Pressure (MPa) | $\Delta_rH_m$* (kJ/mol of $H_2$) | Ref. |
|---|---|---|---|---|---|
| 1 | $B_2H_6(g) + 2LiH(s) \rightarrow 2LiBH_4(s)$ | 120 | 2.7 | -421[&] | [10] |
| 2 | $B(s) + Li(s) + 2H_2(g) \rightarrow LiBH_4(s)$ | 700 | 15 | -95 | [17] |
| 3 | $2B(s) + 2LiH(s) + 3H_2(g) \rightarrow 2LiBH_4(s)$ | 400 | 35 | -67 | [15] |
| 4 | $LiB_3(s) + 2LiH(s) + 5H_2(g) \rightarrow 3LiBH_4(s)$ | 700 | 15 | -74 | [17] |
| 5 | $Li_7B_6(s) + 2B + LiH(s) + 31/2H_2(g) \rightarrow 8LiBH_4(s)$ | 700 | 15 | -91 | [17] |
| 6 | $MgB_2(s) + 2LiH(s) + 4H_2(g) \rightarrow 2LiBH_4(s) + MgH_2(s)$ | 265 | 9 | -46 | [22] |
| 7 | $MgB_2(s) + 2LiF(s) + 4H_2(g) \rightarrow 2LiBH_4(s) + MgF_2(s)$ | 390 | 6 | -45 | [26, 27] |
| 8 | $SiB_4(s) + 4LiH(s) + 6H_2(g) \rightarrow 4LiBH_4(s) + Si(s)$ | 250 | 10 | -65 | this study |
| 9 | $SiB_4(s) + 4LiF(s) + 8H_2(g) \rightarrow 4LiBH_4(s) + SiF_4(g)$[#] | 400 | 12 | 13 | this study |
| 10 | $2FeB(s) + 2LiH(s) + 3H_2(g) \rightarrow 2LiBH_4(s) + 2Fe(s)$[#] | 400 | 10 | -19 | this study |
| 11 | $FeB(s) + LiF(s) + 2H_2(g) \rightarrow LiBH_4(s) + FeF(g)$[#] | 400 | 10 | 274 | this study |
| 12 | $TiB_2(s) + 2LiH(s) + 4H_2(g) \rightarrow$ | 400 | 10 | -16 | this |

| | | | | | |
|---|---|---|---|---|---|
| | $2LiBH_4(s) + TiH_2(s)^{\#}$ | | | | study |
| 13 | $TiB_2(s) + 2LiH(s) + 3H_2(g) \rightarrow 2LiBH_4(s) + Ti(s)^{\#}$ | 400 | 10 | 27 | this study |
| 14 | $TiB_2(s) + 2LiF(s) + 4H_2(g) \rightarrow 2LiBH_4(s) + TiF_2(s)^{\#}$ | 400 | 10 | 53 | this study |

* our calculated value of molar reaction enthalpy change for the system

& valve unit is kJ/mol of $B_2H_6$ for this system

# only B-H bond formed in these systems under the synthesis conditions of this study

## 2. Experimental section

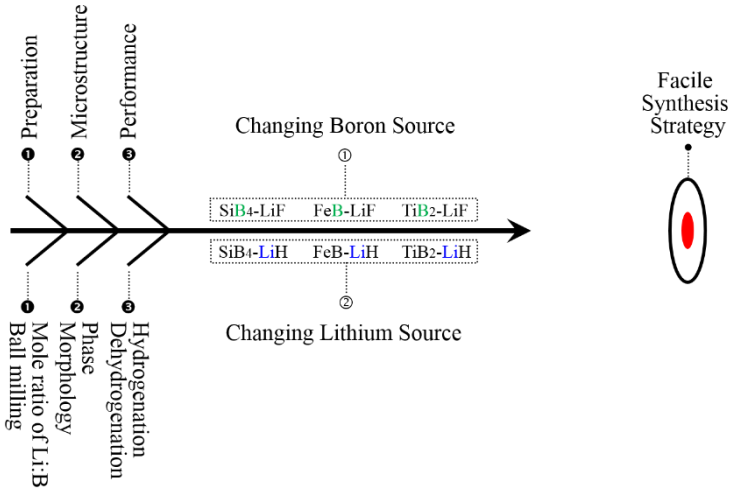


Figure 1 An arrow is tried to shoot the target showing the overview of the experimental section

Figure 1 shows the overview of the experimental section by using a diagrammatic sketch of an arrow trying to shoot the target. Metal borides of $TiB_2$ (Eno Material), FeB (self-prepared), $SiB_4$ (Sigma Aldrich), lithium compounds of LiH (Chemical Reagent Co., Tianjin) and LiF (Sigma Aldrich) were used directly as starting materials. Considering that these raw materials possess diverse particle size which consequently causes the difficulty to clarify the effect of metal borides on the synthesis of $LiBH_4$, these metal borides were firstly milled by a planetary ball milling (QM-3SP2, Nanjing Nanda Instrument Plant) to reduce the particle size into a close nanoscale, as shown in Figure 2. The milling conditions were 40:1 for ball-to-powder ratio, 490 rpm for rotation speed and 150 h ($TiB_2$)/20 h (FeB)/70 h ($SiB_4$) for milling time. Later, those pre-treated metal borides mixing with LiH or LiF was milled by a vibration ball milling (QM-3C,

Nanjing Nanda Instrument Plant). The ball-to-powder ratio was 120:1, rotation speed was 1200 rpm and milling time was 1 h. The samples were sealed in a stainless steel vessel with hardened stainless steel balls and 1 bar Ar gas protection. For synthesizing $LiBH_4$, a stoichiometric ratio of Li:B=1:1 was adopted prior to the milling. In other words, the stoichiometric ratio of each sample was 4:1 for LiF:$SiB_4$ and LiH:$SiB_4$, 1:1 for LiF:FeB and LiH:FeB, 2:1 for LiF:$TiB_2$ and LiH:$TiB_2$. Hydrogenation of these milled samples was executed by a Sievert-type apparatus (PCTPro 2000, Setaram) at conditions of a hydrogen pressure of 10 or 12 MPa, a temperature of 250 or 400 ºC and holding hours of 10 or 16 h.

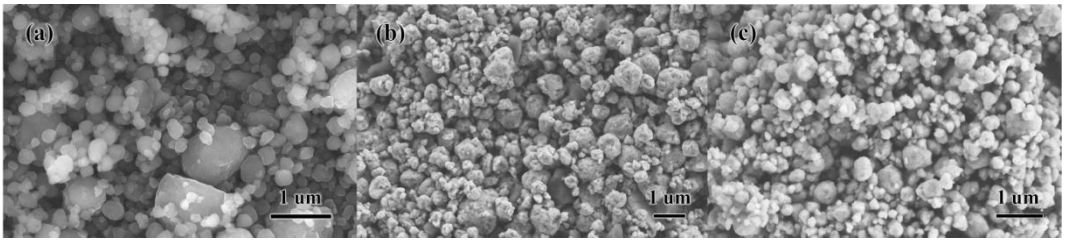


Figure 2 SEM morphologies of milled $SiB_4$ (a), FeB (b) and $TiB_2$ (c). The bulk metal borides were pulverized into nanosized particles having a close scale, which allowed one to eliminate the size effect on puzzling the understanding of their hydrogenation performances.

The morphologies of the pre-treated metal borides were observed by a scanning electron microscopy (SEM, Zeiss-Supra 40). Temperature programmed desorption mass spectrometry (TPD-MS, Hiden Qic20) was used to detect gaseous species released from the hydrogenated samples by heating from 50 ºC to 700 ºC at a heating rate of 4 ºC/min with Ar purge rate of 60 mL/min. The dehydrogenation capacity was measured by a Sievert-type apparatus (PCT Pro 2000, Setaram) at 400 ºC under static vacuum, and the value was calculated with respect to total amount of hydrogenated sample. X-ray diffraction measurements (XRD) were performed on a Philips X'Pert X-ray diffractometer (Cu Kα radiation, tube parameters: V=40 kV, I=40 mA) to characterize the phases in the hydrogenated and dehydrogenated samples. The samples were covered with a 3M film to prevent contamination, which engenders a scattering peak at $2\theta \approx 18^{\circ}$ in

the patterns. Fourier transform infrared spectra (FTIR, Vector 33; Bruker) were recorded from 32 scans of pressed KBr pellets at 3000-1000 $cm^{-1}$ with a 4 $cm^{-1}$ resolution. The background signal was subtracted from sample spectra. All the samples were handled in glove-box filled with high purity Ar gas (99.999%), and the $H_2O$ and $O_2$ level were less than 3 ppm.

## 3. Results and Discussion

### 3.1 Hydrogenation performance

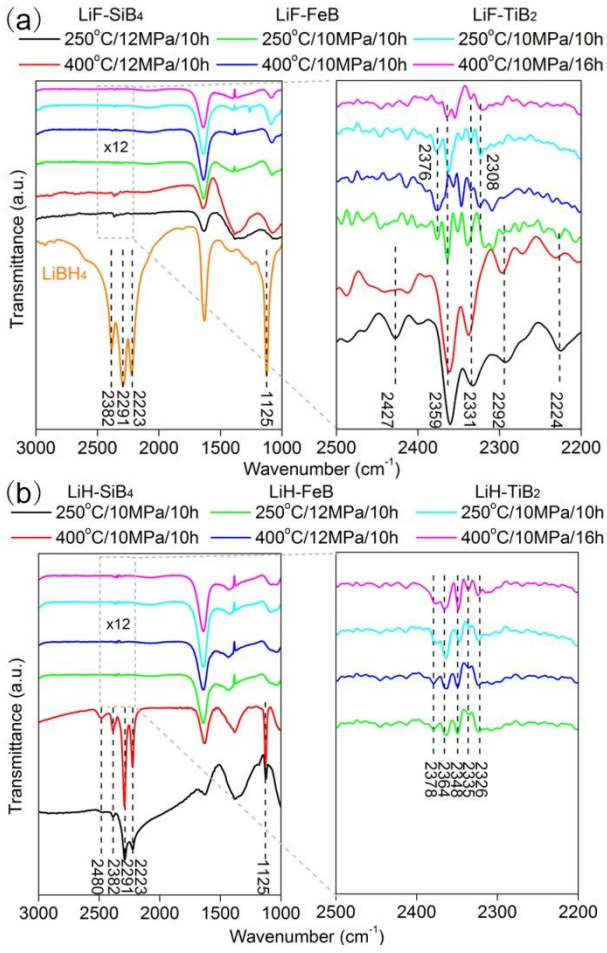


Figure 3 FTIR spectra of $SiB_4$/FeB/$TiB_2$-LiF (a) and $SiB_4$/FeB/$TiB_2$-LiH (b) after hydrogenation at different conditions. The right part is the enlargement of the dashed region in left FTIR. B-H bond vibrations were observed in all samples, and B-H vibrations with strong intensity were only detected in hydrogenated $SiB_4$ mixing with LiF or LiH.

Figure 3 shows the FTIR spectra of $SiB_4$, FeB, and $TiB_2$ mixing with LiF or LiH after hydrogenation which reveals their feasibility for generating $LiBH_4$. For the hydrogenated samples of $SiB_4$/FeB/$TiB_2$-LiF, several B-H bond vibration peaks located mainly between 2200 and 2500

$cm^{-1}$ were observed, which was very close to the bond vibrations at 2382, 2291 and 2223 $cm^{-1}$ of commercial $LiBH_4$[29, 30]. This result indicates that a fragment of B-H bonds was successfully formed in those hydrogenated samples. The weaken vibration intensity of these bonds declared that the amounts of B-H bonds were in a small quantity possibly due to the reaction barrier restricting the combination of boron and hydrogen atoms. Furthermore, alternating the synthesis parameters of temperature, hydrogen pressure and holding time seemed to show limited influence on facilitating the formation of B-H bonds, which was indicated by the similar vibration intensity of B-H bonds. Whereas, the peak intensity of B-H bonds of the hydrogenated $SiB_4$-LiF sample was obviously stronger than that of the other two samples, revealing that the B-H bonds were prone to be formed much more easily. These results indicate the chemical state of boron certainly affects the formation of B-H bonds and the subsequent yield of $LiBH_4$. For these hydrogenated samples, it is noticeable that the peak locations of the B-H bonds were different from that of commercial $LiBH_4$, which indicates that the formation of $[BH_4]^-$ anion was not achieved and it therefore did not result in the generation of $LiBH_4$ successfully. However, this result implies that the formation of $LiBH_4$ was a stepwise process possibly like $LiBH_{4-x} \rightarrow LiBH_4$, in which the hydrogen atoms were gradually absorbed by the hydrogen-deficient anion $[BH_{4-x}]^-$ to form the intact $[BH_4]^-$ anion[31]. The synthesis performance of $SiB_4$/FeB/$TiB_2$-LiF systems is unsatisfactory at the moderate hydrogenation conditions in this work in contrast to the reported systems[10, 15, 17, 22]. It should be ascribed to their positive reaction enthalpy change, as shown in Table 1, that restricted the occurrence of hydrogenation reaction. By changing LiF into LiH which possesses a lower bond dissociation energy ($\Delta_f H_{298}$=247 kJ/mol) than that of LiF ($\Delta_f H_{298}$=577 kJ/mol), the reaction process for synthesizing $LiBH_4$ would be enhanced.

For hydrogenated samples of $SiB_4$/FeB/$TiB_2$-LiH, the vibration peaks locating between 2200 and 2500 $cm^{-1}$ indicated the formation of B-H bonds. Among these samples, the B-H bond vibrations of the hydrogenated FeB/$TiB_2$-LiH samples were in a weakened peak profile, and their peak locations were different from that of commercial $LiBH_4$. This result, again, suggests that the boron source in the state of FeB/$TiB_2$ is too stable to give birth to $[BH_4]^-$ anion. It should be arisen from that FeB/$TiB_2$-LiH systems has higher negative reaction enthalpy change in comparison with other reported systems of metal borides reacting with LiH, as shown in Table 1. Harsh hydrogenation conditions may be necessary to overcome the reaction restriction and therefore promote the synthesis process to generate $LiBH_4$. Importantly, in the example of the hydrogenated $SiB_4$-LiH sample, the characteristic B-H stretching vibration peaks at 2382, 2291, 2223 $cm^{-1}$ and bending vibration peak at 1125 $cm^{-1}$ with strong peak intensity were clearly observed, which are in a good agreement with that of commercial $LiBH_4$. This result indisputably declares that, owing to a boron state different from FeB and $TiB_2$, $SiB_4$ effectively facilitated the formation of $LiBH_4$. In addition to those aforementioned B-H bond vibrations, another B-H bond vibration peak at 2480 $cm^{-1}$ was also detected and it was accordingly assigned to an intermediate phase $Li_{12}B_{12}H_{12}$[29, 32]. The peak intensity of B-H vibration in the hydrogenated $SiB_4$-LiH sample was found to be greatly enhanced when the temperature was increased from 250 °C to 400 °C that it indicates the incremental yield of $LiBH_4$. It is worthwhile to point out that, in this work, the employed temperature and hydrogen pressure as low as 250 °C and 10 MPa for $SiB_4$-LiH system is comparable to that of other reported systems due to it possesses a preferable reaction enthalpy change as summarized in Table 1. This demonstrates an effective synthesis way targeting $LiBH_4$ through $SiB_4$-LiH system hydrogenated at moderate conditions. Later, the

dehydrogenation behavior of the hydrogenated $SiB_4$-LiH was also investigated and the results were shown in the following section.

3.2 Dehydrogenation performance

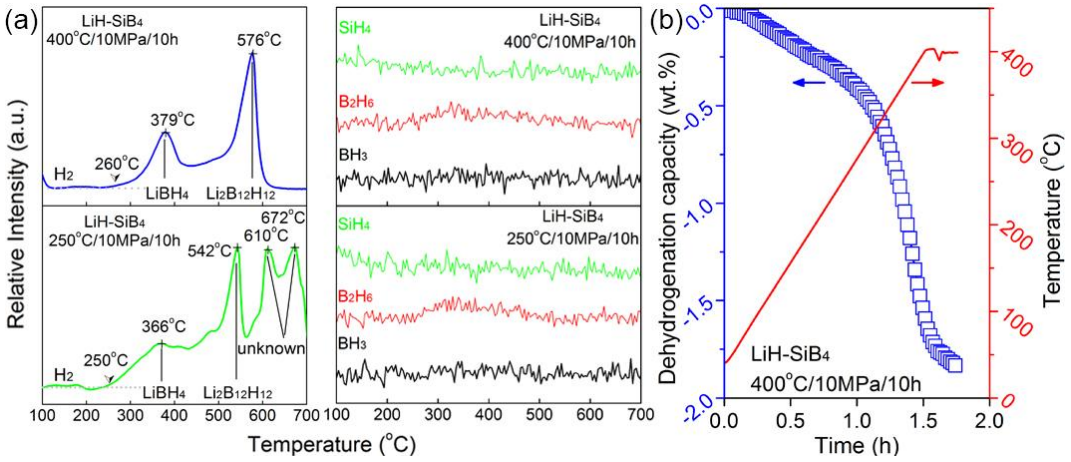


Figure 4 TPD-MS (a) and isothermal dehydrogenation curve at 400 °C (b) of $SiB_4$-LiH samples after hydrogenation at different conditions. Pure hydrogen was liberated and the dehydrogenation peaks revealed the complex dehydrogenation processes.

Figure 4 shows the TPD-MS of gaseous species evolution of $H_2$, $BH_3$, $B_2H_6$ and $SiH_4$, and the isothermal dehydrogenation curve of the hydrogenated $SiB_4$-LiH samples. It is clear that pure hydrogen was released from the hydrogenated samples without any other by-products. For the sample hydrogenated at 250 °C, its dehydrogenation started at 250 °C and reached the first peak at 366 °C accompanying with three stronger peaks at 542, 610 and 672 °C. For the sample hydrogenated at 400 °C, its dehydrogenation initiated from 260 °C and showed two distinct peaks at 379 and 576 °C. Combining with the FTIR results in Figure 3 which revealed the coexistence of $LiBH_4$ and $Li_{12}B_{12}H_{12}$ in those two samples, the peaks at 366 and 379 °C should originate from the dehydrogenation of $LiBH_4$, while the peaks at 542 and 576 °C resulted from the dehydrogenation of $Li_{12}B_{12}H_{12}$. The peaks at higher temperatures of 610 and 672 °C stemmed from the dehydrogenation of hydrogen-containing phases having higher thermodynamic stability. One of them should be ascribed to the dehydrogenation of LiH which dehydrogenates at a high

225 temperature of 720°C[33]. Another one was from unknown compound(s), whereas intermediate
226 phases of $Li_2B_nH_n$ ($n$=5-11) and $LiB_3H_3$ were excluded due to their lower thermodynamic stability
227 predicted by the result of computational study[34].

228 Herein, three important points relating to an understanding of the dehydrogenation behavior
229 of hydrogenated $SiB_4$-LiH are necessary to be clarified. Firstly, as we all know, the
230 dehydrogenation of $LiBH_4$ itself starts at 280 °C and reaches a peak temperature of 480 °C, while
231 the intermediate phase $Li_{12}B_{12}H_{12}$ is supposed to dehydrogenate at 696 °C[35]. In the
232 hydrogenated LiH-$SiB_4$ samples, the dehydrogenation of $LiBH_4$ and $Li_{12}B_{12}H_{12}$ took place at
233 lower temperatures as indicated in Figure 4a. The reason for this temperature reduction is
234 originated from a destabilization reaction between the $LiBH_4$ (or $Li_{12}B_{12}H_{12}$) and hydrogenating
235 products which was discussed in the following. Secondly, it is noticeable that both the onset and
236 peak dehydrogenation temperatures went up to higher region when the $SiB_4$-LiH sample was
237 hydrogenated at higher temperature. This should be ascribed to a higher thermodynamic stability
238 of $LiBH_4$ and $Li_{12}B_{12}H_{12}$ resulting from their further formation and particle growth at elevated
239 hydrogenation temperature. Lastly, a phenomenon of phase transformation took place during the
240 dehydrogenation of $LiBH_4$. In the example of $SiB_4$-LiH hydrogenated at 400 °C and 10 MPa, the
241 amount of $LiBH_4$ is higher than that of $Li_{12}B_{12}H_{12}$ as revealed by the peak area difference in FTIR
242 spectrum (see Figure 3). However, in the TPD-MS curve, the result is opposite to the
243 above-mentioned one as the peak area of $Li_{12}B_{12}H_{12}$ was larger than that of $LiBH_4$. The sole
244 explanation is that less amount of $Li_{12}B_{12}H_{12}$ was generated after hydrogenation treatment of
245 $SiB_4$-LiH sample, while higher amount of this intermediate phase formed during the
246 dehydrogenation of $LiBH_4$[36]. To quantify the synthesized $LiBH_4$ in the $SiB_4$-LiH sample

hydrogenated at 400 °C and 10 MPa, dehydrogenation capacity measurement was carried out at 400 °C. This temperature is selected according to the result of TPD-MS in which the dehydrogenation of $LiBH_4$ almost finished at this point. An estimated value of 19.6 wt.% $LiBH_4$ was obtained through the calculation according to the dehydrogenation capacity of 1.8 wt.% hydrogen. Although the yield is lower in this situation probably due to the kinetic barrier of the hydrogenation reaction, the $SiB_4$-LiH system still has a strong potential for synthesizing $LiBH_4$. For realizing it, the technical issues of material preparation of $SiB_4$ and LiH (for example, finest particle to enhance atoms transferring) and synthesis procedure optimization (heating temperature/hydrogen pressure/soaking time) are considered in our future work to acquire higher yield of $LiBH_4$, and further developing this promising candidate as hydrogen storage material.

3.3 Microstructure after hydrogenation and dehydrogenation

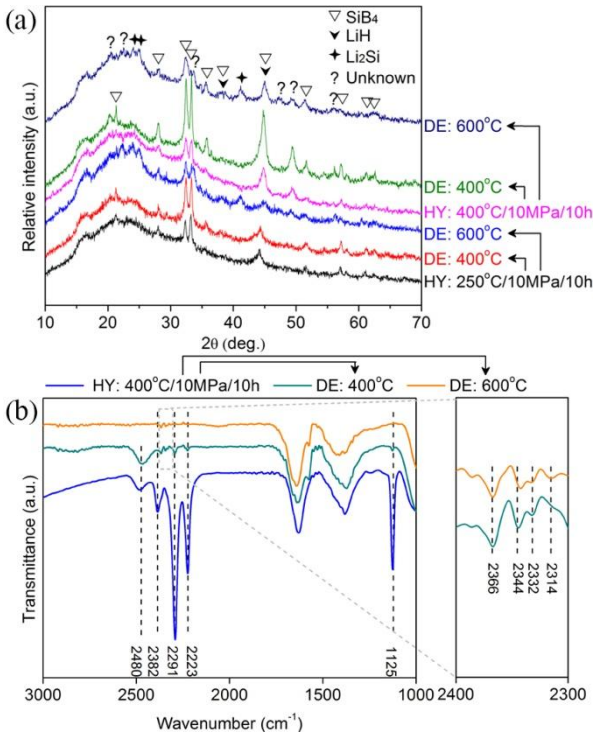


Figure 5 XRD patterns (a) and FTIR spectra (b) of $SiB_4$-LiH samples after hydrogenation (HY) and subsequent dehydrogenation (DE) at different temperatures as directed by the arrows. The synthesized $LiBH_4$ had an amorphous structure in hydrogenated $SiB_4$-LiH, and its destabilized dehydrogenation pathway was proposed.

Figure 5 shows the XRD patterns and FTIR spectra of $SiB_4$-LiH samples after hydrogenation and subsequent dehydrogenation. (i) When hydrogenation treatment took place either at lower temperature of 250 °C or higher temperature of 400 °C, only the diffraction peaks of $SiB_4$ were observed in the XRD patterns in Figure 5 (a), and the B-H bond vibration peaks of $LiBH_4$ and $Li_2B_{12}H_{12}$ were clearly observed in the FTIR spectra in Figure 5 (b). This indicates the synthesized $LiBH_4$ and intermediate phase $Li_2B_{12}H_{12}$ are in an amorphous state which resulted in their invisible diffraction peaks in the corresponding XRD patterns. In our previous works, it was found that $Li_2B_{12}H_{12}$ could be rehydrogenated into $LiBH_4$ at certain hydrogenation conditions[37, 38]. Thus, for the $SiB_4$-LiH system, one can speculate that $SiB_4$ reacted with LiH to generate $Li_{12}B_{12}H_{12}$ under hydrogen atmosphere, and this intermediate phase was subsequently hydrogenated into $LiBH_4$. The overall hydrogenation reaction pathway for the $SiB_4$-LiH system was proposed as shown in equation (3) in the following. In the reported works, the formation of $Li_{12}B_{12}H_{12}$ via the reaction between $LiBH_4$ and $B_2H_6$ was confirmed during the synthesis process of $LiBH_4$[10, 39]. According to this, it cannot rule out the formation of $B_2H_6$ during the hydrogenation process of $SiB_4$-LiH, which gave birth to the formation of $Li_{12}B_{12}H_{12}$. The $B_2H_6$ species possibly originated from the reaction between $H_2$ and B which was set free from $SiB_4$ similar to the finding in the example of hydrogenating LiB[18]. Hydrogenating product Si should be in an amorphous state, which resulted in its undetectable diffraction peaks in the XRD patterns.

(ii) When those two hydrogenated samples dehydrogenated at 400 °C, several weaken diffraction peaks of unknown phase(s) were observed in the XRD patterns in Figure 5 (a), and the diffraction peak intensity of $SiB_4$ at around $2\theta=32°$ became sharper which indicated its crystalline growth. As reported by previous works, metals could react with $LiBH_4$ to form metal hydrides or

metal borides[40, 41]. However, $SiH_4$ was not detected during the dehydrogenation of hydrogenated $SiB_4$-LiH samples as revealed by the TPD-MS result (see Figure 4a). Thus, it was speculated that the crystalline growth of $SiB_4$ was originated from the new generation of $SiB_4$. This should be originated from that the in-situ formed Si metal in the hydrogenated sample reacted with $LiBH_4$ and therefore produced the new $SiB_4$ substance. This destabilization reaction consequently resulted in the reduction of dehydrogenation temperature of $LiBH_4$, as shown in Figure 4a. It is noticeable that the unknown phase(s) with weaken diffraction intensity were found in the dehydrogenated samples. The formation of intermediate phase $Li_{12}B_{12}H_{12}$ was confirmed during the dehydrogenation of $LiBH_4$ as formerly revealed in the FTIR spectrum and TPD-MS results (see Figure 3 and 4). Consequently, the dehydrogenation pathway of $LiBH_4$ at 400 °C is proposed as shown in equation (4a).

(iii) When the sample dehydrogenated at 600 °C, $Li_{12}B_{12}H_{12}$ was completely consumed as revealed by the absence of vibration peak at 2480 $cm^{-1}$ in FTIR spectrum in Figure 5(b). It was also found that the diffraction intensity of $SiB_4$ decreased in the XRD pattern at this higher temperature, while diffraction peaks of LiH, $Li_2Si$ and unknown phase(s) were clearly observed. Thus, it is speculated that $Li_{12}B_{12}H_{12}$ reacted with $SiB_4$ and therefore leading to the formation of those products. A possible dehydrogenation reaction is proposed as shown in equation (4b). Combining with the FTIR results in Figure 5 that several new B-H vibrations were identified between 2400 and 2300 $cm^{-1}$, the unknown phase(s) should be the intermediate compounds which dehydrogenated from $LiBH_4$ and/or $Li_2B_{12}H_{12}$, and released hydrogen at higher temperatures as indicated by the results of TPD-MS in Figure 4a. Further investigation will be carried on to figure out the unknown phase(s).

307 Hydrogenation reaction:

308 $$SiB_4(s) + 4LiH(s) + 6H_2(g) \rightarrow 4LiBH_4(s) + Si(s) \quad (3)$$

309 Dehydrogenation reaction:

310 $$LiBH_4(s) + Si(s) \rightarrow LiH(s) + Li_2B_{12}H_{12}(s) + SiB_4(s) + H_2(g) + \text{unknown phase(s)} \quad 400\ ^\circ C \quad (4a)$$

311 $$Li_2B_{12}H_{12}(s) + SiB_4(s) \rightarrow LiH(s) + Li_2Si(s) + H_2(g) + \text{unknown phase(s)} \quad 600\ ^\circ C \quad (4b)$$

312 **4. Conclusion**

313 The formation of B-H bonds in $[BH_4]^-$ anion remarkably determines the generation of $LiBH_4$.
314 Thus, FeB, $TiB_2$ and $SiB_4$ which have a chemical state of boron different from elemental B were
315 used to investigate the facilitation of B-H bond formation towards the easy synthesis of $LiBH_4$.
316 The $SiB_4$/FeB/$TiB_2$-LiF/LiH systems showed their different capability of forming B-H bonds
317 when they were subjected to a hydrogenation treatment. The systems of FeB/$TiB_2$ mixing with
318 LiF/LiH gave birth to fewer amounts of B-H bonds, whereas the $SiB_4$ preferably facilitated the
319 formation of B-H bonds either reacting with LiF or LiH. Particularly, $SiB_4$-LiH system exhibited
320 the best performance for synthesizing $LiBH_4$ at moderate conditions of 250 °C and 10 MPa $H_2$,
321 and this reaction can be promoted by increasing the temperature to 400 °C. A hydrogenation
322 reaction pathway, $SiB_4(s) + 4LiH(s) + 6H_2(g) \rightarrow 4LiBH_4(s) + Si(s)$, was proposed according to the
323 experimental result. Besides, a stepwise hydrogen absorption process of $LiBH_{4-x} \rightarrow LiBH_4$ possibly
324 took place during the hydrogenation. The dehydrogenation behavior of the hydrogenated $SiB_4$-LiH
325 system was also studied and the speculated reaction pathway was shown in this work. The
326 hydrogenation synthesis approach using $SiB_4$ as boron source may be also applicable for other
327 promising tetrahydroborates, such as $Ca(BH_4)_2$ or $Mg(BH_4)_2$, for which LiH is replaced by $CaH_2$
328 or $MgH_2$, respectively.

**Acknowledgments**

This work was supported by the National Natural Science Foundation of China (grant number 21805046), the Public Welfare Research and Capacity Building Project of Guangdong (grant number 2015A010105028), the Open Fund of the Guangdong Provincial Key Laboratory of Advance Energy Storage Materials, Project of "One-Hundred Young Talents" of Guangdong University of Technology (grant number 220413551), and the PolyU Departmental General Research Grant (no. G-UADK).

## References


[1] R. S. Middleton; R. Gupta; J. D. Hyman; H. S. Viswanathan, The shale gas revolution: Barriers, sustainability, and emerging opportunities. *Applied Energy*, 2017. **199**: 88-95.

[2] H. Wang; H. J. Lin; W. T. Cai; L. Z. Ouyang; M. Zhu, Tuning kinetics and thermodynamics of hydrogen storage in light metal element based systems – A review of recent progress. *Journal of Alloys and Compounds*, 2016. **658**: 280-300.

[3] S. J. Qiu; H. L. Chu; Y. J. Zou; C. L. Xiang; F. Xu; L. X. Sun, Light metal borohydrides/amides combined hydrogen storage systems: composition, structure and properties. *Journal of Materials Chemistry A*, 2017. **5**(48): 25112-25130.

[4] T. He; P. Pachfule; H. Wu; Q. Xu; P. Chen, Hydrogen carriers. *Natrue Reviews Matrials*, 2016. **1**(12).

[5] Qilu Yao; Weimei Shi; Gang Feng; Zhanghui Lu; Xiaoliang Zhang; Duanjian Tao; Dejing Kong; Xiangshu Chen, Ultrafine Ru nanoparticles embedded in $SiO_2$ nanospheres: Highly efficient catalysts for hydrolytic dehydrogenation of ammonia borance. *Journal of Power Sources*, 2014. **257**: 293-299.

[6] Zhujun Zhang; Zhanghui Lu; Hongliang Tan; Xiangshu Chen; Qilu Yao, $CeO_x$-modified RhNi nanoparticles grown on rGo as highly efficient catalysts for complete hydrogen generation from hydrazine borane and hydrazine. *Journal of Materials Chemistry A*, 2015. **3**(46): 23520-23529.

[7] H. Q. Kou; W. H. Luo; Z. Y. Huang; R. Li; G. Sang; T. Tang; G. H. Zhang; C. G. Chen; C. W. Hu; Y. L. Zhou, Verification and kinetics analysis on the synthesis of $LiBH_4$ from $LiH+MgB_2$. *International Journal of Hydrogen Energy*, 2016. **41**(26): 11293-11300.

[8] H. C. Brown; Y. M. Choi; S. Narasimhen, Convenient procedure for the conversion of sodium borohydride into lithium borohydride in simple ether solvents. *Inorganic Chemistry*, 1981. **20**(12): 4454-4456.

[9] R. Gremaud; A. Borgschulte; O. Friedrichs; A. Züttel, Synthesis mechanism of alkali borohydrides by heterolytic diborane splitting. *The Journal of Physical Chemistry C*, 2011. **115**(5): 2489-2496.

[10] O. Friedrichs; A. Borgschulte; S. Kato; F. Buchter; R. Gremaud; A. Remhof; A. Züttel, Low-temperature synthesis of $LiBH_4$ by gas–solid reaction. *Chemistry – A European Journal*, 2009. **15**(22): 5531-5534.

[11] O. Friedrichs; J. W. Kim; A. Remhof; D. Wallacher; A. Hoser; Y. W. Cho; K. H. Oh; A. Züttel, Core shell structure for solid gas synthesis of $LiBD_4$. *Physical Chemistry Chemical Physics*, 2010. **12**(18): 4600-4603.

[12] O. Friedrichs; A. Remhof; A. Borgschulte; F. Buchter; S. I. Orimo; A. Züttel, Breaking the passivation-the road to a solvent free borohydride synthesis. *Physical Chemistry Chemical Physics*, 2010. **12**(36): 10919-10922.

[13] A. Remhof; A. Borgschulte; O. Friedrichs; P. Mauron; Y. Yan; A. Züttel, Solvent-free synthesis and decomposition of $Y(BH_4)_3$. *Scripta Materialia*, 2012. **66**(5): 280-283.

[14] S. Orimo; Y. Nakamori; G. Kitahara; K. Miwa; N. Ohba; S. Towata; A. Züttel, Dehydriding and rehydriding reactions of $LiBH_4$. *Journal of Alloys and Compounds*, 2005. **404**: 427-430.

[15] R. Chen; X. H. Wang; L. Xu; H. Li; C. P. Chen; L. X. Chen; H. G. Pan, Direct preparation of $LiBH_4$ from pre-treated LiH+B mixture at high pressure. *Journal of Alloys and Compounds*, 2011. **509**(8): 3481-3485.

[16] F. Agresti; A. Khandelwal, Evidence of formation of $LiBH_4$ by high-energy ball milling of LiH and B in a hydrogen atmosphere. *Scripta Materialia*, 2009. **60**(9): 753-755.
[17] O. Friedrichs; F. Buchter; A. Borgschulte; A. Remhof; C. N. Zwicky; P. Mauron; M. Bielmann; A. Züttel, Direct synthesis of $LiBH_4$ and $LiBD_4$ from the elements. *Acta Materialia*, 2008. **56**(5): 949-954.
[18] A. Remhof; O. Friedrichs; F. Buchter; P. Mauron; A. Züttel; D. Wallacher, Solid-state synthesis of $LiBD_4$ observed by in situ neutron diffraction. *Physical Chemistry Chemical Physics*, 2008. **10**(38): 5859-5862.
[19] Ç. Çakanyıldırım; M. Gürü, Processing of $LiBH_4$ from its elements by ball milling method. *Renewable Energy*, 2008. **33**(11): 2388-2392.
[20] J. J. Vajo; S. L. Skeith; F. Mertens, Reversible storage of hydrogen in destabilized $LiBH_4$. *The Journal of Physical Chemistry B*, 2005. **109**(9): 3719-3722.
[21] G. Barkhordarian; T. Klassen; M. Dornheim; R. Bormann, Unexpected kinetic effect of $MgB_2$ in reactive hydride composites containing complex borohydrides. *Journal of Alloys and Compounds*, 2007. **440**(1-2): L18-L21.
[22] L. L. Shaw; X. F. Wan; J. Z. Hu; J. H. Kwak; Z. G. Yang, Solid-state hydriding mechanism in the $LiBH_4$ + $MgH_2$ system. *The Journal of Physical Chemistry C*, 2010. **114**(17): 8089-8098.
[23] Y. Zhang; F. Morin; J. Huot, The effects of Ti-based additives on the kinetics and reactions in LiH/$MgB_2$ hydrogen storage system. *International Journal of Hydrogen Energy*, 2011. **36**(9): 5425-5430.
[24] I. Saldan; R. Campesi; O. Zavorotynska; G. Spoto; M. Baricco; A. Arendarska; K. Taube; M. Dornheim, Enhanced hydrogen uptake/release in 2LiH-$MgB_2$ composite with titanium additives. *International Journal of Hydrogen Energy*, 2012. **37**(2): 1604-1612.
[25] U. Bösenberg; J. W. Kim; D. Gosslar; N. Eigen; T. R. Jensen; J. M. B. von Colbe; Y. Zhou; M. Dahms; D. H. Kim; R. Günther, Role of additives in $LiBH_4$–$MgH_2$ reactive hydride composites for sorption kinetics. *Acta Materialia*, 2010. **58**(9): 3381-3389.
[26] I. Saldan; R. Gosalawit-Utke; C. Pistidda; U. Bösenberg; M. Schulze; T. R. Jensen; K. Taube; M. Dornheim; T. Klassen, Influence of stoichiometry on the hydrogen sorption behavior in the LiF–$MgB_2$ system. *The Journal of Physical Chemistry C*, 2012. **116**(12): 7010-7015.
[27] R. Gosalawit-Utke; J. M. B. von Colbe; M. Dornheim; T. R. Jensen; Y. Cerenius; C. Bonatto Minella; M. Peschke; R. Bormann, LiF−$MgB_2$ system for reversible hydrogen storage. *The Journal of Physical Chemistry C*, 2010. **114**(22): 10291-10296.
[28] I. Saldan; M. Schulze; C. Pistidda; R. Gosalawit-Utke; O. Zavorotynska; L. H. Rude; J. Skibsted; D. Haase; Y. Cerenius; T. R. Jensen, et al., Hydrogen sorption in the LiH-LiF-$MgB_2$ system. *Journal of Physical Chemistry C*, 2013. **117**(33): 17360-17366.
[29] M. P. Pitt; M. Paskevicius; D. H. Brown; D. A. Sheppard; C. E. Buckley, Thermal stability of $Li_2B_{12}H_{12}$ and its role in the decomposition of $LiBH_4$. *Journal of the American Chemical Society*, 2013. **135**(18): 6930-6941.
[30] W. T. Cai; Juner Chen; L. Y. Liu; Y. Z. Yang; H. Wang, Tuning the structural stability of $LiBH_4$ through boron-based compounds towards superior dehydrogenation. *Journal of Materials Chemistry A*, 2018. **6**(3): 1171-1180.
[31] A. Züttel; P. Wenger; S. Rentsch; P. Sudan; P. Mauron; C. Emmenegger, $LiBH_4$ a new hydrogen storage material. *Journal of Power Sources*, 2003. **118**(1-2): 1-7.
[32] B. Richter; D. B. Ravnsbæk; M. Sharma; A. Spyratou; H. Hagemann; T. R. Jensen, Fluoride

425 substitution in $LiBH_4$; destabilization and decompostion. *Physical Chemistry Chemical*
426 *Physics*, 2017. **44**(19):30157-30165.
427 [33] W. Grochala; P. P. Edwards, Thermal decomposition of the non-interstitial hydrides for the
428 storage and production of hydrogen. *Chemical Reviews*, 2004. **104**(3): 1283-1315.
429 [34] N. Ohba; K. Miwa; M. Aoki; T. Noritake; S. I. Towata; Y. Nakamori; S. I. Orimo; A. Züttel,
430 First-principles study on the stability of intermediate compounds of $LiBH_4$. *Physical Review*
431 *B*, 2006. **74**(7): 075110.
432 [35] V. Ozolins; E. H. Majzoub; C. Wolverton, First-principles prediction of thermodynamically
433 reversible hydrogen storage reactions in the Li-Mg-Ca-B-H System. *Journal of the American*
434 *Chemical Society*, 2009. **131**(1): 230-237.
435 [36] Y. G. Yan; A. Remhof; S. J. Hwang; H. W. Li; P. Mauron; S. I. Orimo; A. Züttel, Pressure and
436 temperature dependence of the decomposition pathway of $LiBH_4$. *Physical Chemistry*
437 *Chemical Physics*, 2012. **14**(18): 6514-6519.
438 [37] W. T. Cai; H. Wang; J. W. Liu; L. F. Jiao; Y. J. Wang; L. Z. Ouyang; T. Sun; D. L. Sun; H. H.
439 Wang; X. D. Yao; et al., Towards easy reversible dehydrogenation of $LiBH_4$ by catalyzing
440 hierarchic nanostructured CoB. *Nano Energy*, 2014. **10**: 235-244.
441 [38] Y. G. Yan; H. Wang; M. Zhu; W. T. Cai; D. Rentsch; A. Remhof, Direct rehydrogenation of
442 $LiBH_4$ from H-deficient $Li_2B_{12}H_{12-x}$. *Crystals*, 2018. 8(3):131-137.
443 [39] O. Friedrichs; A. Remhof; S. J. Hwang; A. Züttel, Role of $Li_2B_{12}H_{12}$ for the formation and
444 decomposition of $LiBH_4$. *Chemistry of Materials*, 2010. **22**(10): 3265-3268.
445 [40] J. Yang; A. Sudik; C. Wolverton, Destabilizing $LiBH_4$ with a metal (M = Mg, Al, Ti, V, Cr, or
446 Sc) or metal hydride ($MH_2$, $MgH_2$, $TiH_2$, or $CaH_2$). *Journal of Physical Chemistry C*, 2007.
447 **111**(51): 19134-19140.
448 [41] B. R. S. Hansen; D. B. Ravnsbaek; D. Reed; D. Book; C. Gundlach; J. Skibsted; T. R. Jensen,
449 Hydrogen storage capacity loss in a $LiBH_4$-Al Composite. *Journal Of Physical Chemistry C*,
450 2013. **117**(15): 7423-7432.